

[Click here to view linked References](#)

1  
2  
3  
4  
5  
6  
7  
8  
9  
10  
11  
12  
13  
14  
15  
16  
17  
18  
19  
20  
21  
22  
23  
24  
25  
26  
27  
28  
29  
30  
31  
32  
33  
34  
35  
36  
37  
38  
39  
40  
41  
42  
43  
44  
45  
46  
47  
48  
49  
50  
51  
52  
53  
54  
55  
56

# 3D printed “Starmix®” drug loaded dosage forms for paediatric applications

Nicolaos Scoutaris<sup>1</sup>, Steven A. Ross<sup>1</sup>, Dennis Douroumis<sup>1\*</sup>

<sup>1</sup>Faculty of Engineering and Science, School of Science, University of Greenwich, Chatham  
Maritime, Chatham, Kent ME4 4TB, UK

---

\* Correspondence: Faculty of Engineering and Science, University of Greenwich, Medway Campus,  
Chatham Maritime, Kent ME4 4TB, UK. Tel.: +44 (0) 208 331 8440; Fax: +44 (0) 208 331 9805.  
*E-mail address:* D.Douroumis@gre.ac.uk

57  
58  
59  
60  
61  
62  
63  
64  
65

## ABSTRACT

**Purpose** Three- dimensional (3D) printing has received significant attention as a manufacturing process for pharmaceutical dosage forms. In this study, we used Fusion Deposition Modelling (FDM) in order to print “candy – like” formulations by imitating Starmix® sweets to prepare paediatric medicines with enhanced palatability.

**Methods** Hot melt extrusion processing (HME) was coupled with FDM to prepare extruded filaments of indomethacin (IND), hypromellose acetate succinate (HPMCAS) and polyethylene glycol (PEG) formulations and subsequently feed them in the 3D printer. The shapes of the Starmix® objects were printed in the form of a heart, ring, bottle, ring, bear and lion. Differential scanning calorimetry (DSC), X-ray powder diffraction (XRPD), Fourier Transform Infra-red Spectroscopy (FT-IR) and confocal Raman analysis were used to assess the drug – excipient interactions and the content uniformity.

**Results** Physicochemical analysis showed the presence of molecularly dispersed IND in the printed tablets. *In vivo* taste masking evaluation demonstrated excellent masking of the drug bitterness. The printed forms were evaluated for drug dissolution and showed immediate IND release independently of the printed shape, within 60min.

**Conclusions** 3D printing was used successfully to process drug loaded filaments for the development of paediatric printed tablets in the form of Starmix® designs.

**Keywords:** 3D printing, paediatric medicines, fusion deposition modelling, hot melt extrusion, taste masking

## Abbreviations List

HME	Hot melt extrusion processing
IND	Indomethacin
HPMCAS	Hypromellose acetate succinate
PEG	Polyethylene glycol
DSC	Differential scanning calorimetry
XRPD	X-ray powder diffraction
FT-IR	Fourier Transform Infra-red Spectroscopy
SEM	Scanning Electron Microscopy
HPLC	High performance liquid chromatography
TGA	Thermogravimetric analysis

## INTRODUCTION

The development of high quality, effective and safe paediatric medicines has been proven a challenging process for the pharmaceutical industry. Due to the substantial differences in the drug development process for paediatric patients and adult patients, new regulations were introduced by the European Medicines Agency (EMA) in 2007, which governed the drug production strategies for paediatric medications. According to Strickley et al., (2007) development difficulties are related to dose modification, ease of administration/swallowing, taste masking, physical stability, packaging and providing/designing the measuring device [1].

The oral route of administration is often utilized as the route of choice for the delivery of medical products to paediatric patients, in both solid and liquid forms including; syrups, suspensions and emulsions; powders, granules, effervescent tablets, orodispersible tablets, chewable tablets and gums; mini tablets, innovative granules; and both conventional immediate release and modified release tablets and capsules [2]. A great disadvantage of liquid medications is the higher chance of error when measuring dosage for self-administration. A number of studies have demonstrated that patients who self administer liquid medications have an estimated error rate of 50% to 60%, due to their inability to measure the correct dose [3-5]. This problem can be avoided by manufacturing solid oral dosage forms which offer a number advantages over the liquid forms, these include; having a lower cost of development, easy administration, greater stability, dose accuracy, have the capacity to develop modified release formulations, can be produced with greater uniformity and have greater taste masking capabilities [6]. Although oral administration is the most common route for paediatric populations, the development of palatable formulations is complicated. The developed medicines should be easily swallowed, taste masked while maintaining safety, efficacy, accessibility and affordability. Nevertheless, there is an increased demand for the development of novel technologies for paediatric patients that mainly focus on the formulation design and/or administration/dosing devices [7].

Such a novel technology is 3D printing, which encompasses a wide range of additive manufacture processes, where products are designed using Computer Aided Design (CAD) software [8-11]. The product is then processed by a slicing software that divides the object into thin cross sections. These are then printed out one on top of the other, forming compact layers which form the 3D structure. The primary objective of the various 3D printing technologies is to develop and produce models and prototypes of the designed product in a rapid and inexpensive manner [12]. The epitome of 3D printing applications for medicinal products is the recently approved 3D printed drug product called Spritam (levetiracetam) manufactured by using the Zipdose Technology based on a powder bed—liquid 3D printing technology.

An increasing number of researchers are employing 3D printing technologies to develop oral dosage forms, with modified drug release profiles to allow either sustained or immediate drug release [13-15]. Recently, 3D printing was utilized to create a multi-active solid dosage form, containing 5 different API compartmentalised within the same capsule, which are autonomously controlled with two separate release profiles, called Polypill [16]. An interesting approach was presented by Goyannes *et al.* where an anti-acne drug (salicylic

acid) loaded structure in the shape of a nose was prepared by comparing Fused Deposition Modelling (FDM) and stereolithography [17].

However, FDM has proven to be one of the more versatile 3D printing methods due to the range of potential printing materials, which can be utilized on the system. However, further development of FDM extruders have allowed for the printing of almost any thermoplastic material such as polycarbonate and polyurethane [18]. Recently, the utilisation of FDM was extended to pharmaceutical materials where filaments of drugs and polymers are prepared and extruded through an FDM 3D printer. Specifically, FDM has been utilised to prepare formulations of differing shapes and infill ratio's in order to tune the drug release profile [19, 20]. As expected tablets weights increased with an increasing infill percentage and same size, demonstrating high reproducibility in physical dimensions, along with high mechanical strength which is resistant to damage upon handling. Moreover, extended release tablet of prednisolone were fabricated by using loaded poly(vinyl alcohol) (PVA) filaments [21]. The precision of dose control ranged between 88.7% and 107% while prednisolone existed in amorphous form within the PVA matrix and released from the 3D printed tablet over a 24hr period. Other work involves the development of Patient-Specific Immediate Release Tablets using theophylline loaded filaments as a mixture with PVP in the presence of plasticiser produced by means of hot melt extrusion. A 3D printing technique was applied to produce caplet-shaped tablets with excellent mechanical properties and an immediate *in-vitro* release pattern [22]. The aforementioned examples demonstrate that by simply modifying the printing patterns and structure, without altering the polymer-drug properties, it is possible to modify the drug dissolution rates.

The aim of this work was to introduce the feasibility of 3D printing coupled with hot melt extrusion to prepare paediatric medicines that can be consumed easily by children from 2 – 11 years old. The medicines were designed in such a way to imitate “sweet – like” chewable tablets. Chewable tablets are a valuable paediatric dosage form and have been used for various products such as antacids, antibiotics, anticonvulsants, analgesics, antiasthmatics and cold/allergy preparations. The proposed 3D printing approach improves compliance and adherence of children to the prescribed medication. In addition the combined HME and 3D printing benefits such as taste masking and easy to swallow respectively, lead to dose accuracy and enhanced palatability. For the purposes of the study “Starmix®” (HARIBO PLC, UK) designs were printed using IND as model drug substance and HMPCAS as the polymeric excipient. Indomethacin is a nonsteroidal anti-inflammatory drug commonly used as a prescription medication to reduce fever, pain, stiffness, and swelling from inflammation and HPMCAS is a thermoplastic polymer which has been used primarily as an enteric coating material and dissolves at pH 5.5 – 6.8.

## MATERIALS AND METHODS

### Materials

Indomethacin (IND) and polyethylene glycol (PEG) were purchased from Tokyo Chemicals (Belgium) and Sigma – Aldrich (U.K.) respectively. Hypromellose acetate succinate (HPMCAS, AQOAT AS-MF) was kindly donated by Shin – Etsu (Japan).

### **Extrusion of IND – HPMCAS filament**

1 A physical blend composed of indomethacin, HPMCAS and PEG 6000 at 20/60/20  
2 wt/wt ratio were accurately weighed and homogeneously blended in a Turbula shaker-mixer  
3 at 100rpm for 10 minutes. The blended physical mixer was loaded into a DD Flexwall 18  
4 feeder (Brabender Technology, Germany), and fed into a twin-screw extruder (Eurolab 16,  
5 Thermo Fisher, Germany) at a rate of 10g per minute. A circular shaped die was employed to  
6 yield polymer strand extrudates. The 9 heating zones across the barrel were set at the follow-  
7 ing temperature profile; 40°C, 55°C, 75°C, 100°C, 140°C, 140°C, 140°C, 140°C, 120°C with  
8 the die temperature set at 80°C. The barrel was slightly cooled towards the end to allow the  
9 mixture to re-solidify, ensuring the end-product was extruded as a strand, which is uniform in  
10 diameter. A screw speed of 50 rpm was utilised.

### **3D printing process of paediatric formulations**

16 The Starmix® structures were printed by using a standard FDM printer HD2xR  
17 Airwolf (U.S.A). The structures were designed with SolidWorks (Dassault Systems, USA)  
18 and exported as .stl files which were subsequently imported into Cura software to generate  
19 the Gcode for the printing. The print temperature was 165°C and the print speed was set at  
20 25mm/sec. The infill percentage was 7% and the layer height 150µm. The size of the  
21 perimeter shell was 0.5mm and the top and bottom shell 0.4mm. No supports or rafts were  
22 utilised in the printed model.

### **Scanning Electron Microscopy (SEM)**

28 The morphology of the extruded polymer strands and the 3D printed structure was  
29 observed via scanning electron microscopy (Hitachi SU8030, Japan). Both Samples were  
30 placed on an aluminium stub and coated with a thin layer of Mikrostik nonconductive  
31 adhesive (Agar scientific, UK). The samples were then plated with chromium under an  
32 atmosphere of argon. SEM images were taken using an electron beam accelerating voltage of  
33 2 kV. Images were captured between x30 and 2.00k magnifications.

### **X-Ray Powder Diffraction (XRPD)**

41 X-ray powder diffraction was used to determine the solid state of the bulk materials,  
42 the extruded polymer strand and the polymer strand after 3D Printing. This was done using a  
43 D8 advanced x-ray Diffractometer (Bruker, Germany) in reflection mode. A Cu anode X-ray  
44 tube was powered at 40kV and 40mA. A primary Göbel mirror was used for the parallel  
45 beam and the removal of CuKβ. A primary 4° Soller slit, a secondary 2.5° Soller slit and a  
46 0.6mm exit slit was selected for this experiment. Each sample was scanned from 2 to 60° 2θ  
47 with a step size of 0.02° 2θ degrees/step and a counting time of 0.2 sec/step. As the polymer  
48 samples were difficult to crush to a small enough size to run for XRPD, they were first  
49 doused in liquid nitrogen then ground in a mortar and pedestal, before being placed in a low  
50 background holder and inserted into the device. DIFFRAC.EVA software was used for the  
51 phase analysis.

### **Differential Scanning Calorimetry (DSC)**

57 The temperature profiles of the bulk ingredients and extruded strands were analysed  
58 using a differential scanning calorimeter (Mettler-Toledo 823e, Greifensee, Switzerland). The  
59  
60  
61  
62  
63  
64  
65

1 samples were accurately weighed between 3mg-5mg and placed into an aluminium pan and  
2 crimped. Each sample was heated from 0°C to 300°C at 10°C/min heating rate except for  
3 PEG 6000 which was heated to 150°C. Nitrogen gas was used as a purge, at a flow rate was  
4 set at 50ml/min. STAR excellence software was used to analyse the data.  
5

### 6 **Fourier Transform Infra-red Spectroscopy (FT-IR)**

7 FTIR analysis was performed on the drug, carrier, drug/carrier physical mixtures, and  
8 complex using PerkinElmer PE1600 (Massachusetts 02451, USA) Fourier transform infrared  
9 spectra according to the KBr disc method from 400 to 3600 wavelength/cm<sup>-1</sup> range. For FT-  
10 IR analysis, amorphous IND was prepared by using solvent evaporation method where IND  
11 dissolved in methanol following by rapid evaporation of the solvent.  
12  
13  
14  
15

### 16 **Confocal Raman analysis**

17 Room temperature Raman spectra of the “pure” formulation components were  
18 obtained using a Jobin/Yvon LabRam 320 instrument equipped with an Olympus microscope  
19 (Horiba, Japan). The spectrometer is equipped with an 1800 grooves/mm holographic grating,  
20 a holographic notch filter, a Peltier-cooled CCD (MPP1 chip) for detection, and an Olympus  
21 BX40 microscope. An Ar<sup>+</sup> ion laser ( $\lambda = 633$  nm) was used. Raman spectra of solid-state  
22 samples were collected at room temperature on a microscope slide using a microscope  
23 objective of 50× magnification to focus the laser beam. A backscattering (180° between  
24 excitation and collection) geometry was used in all experiments. Each spectral scan was  
25 collected for 5 s using 4 accumulations. The Raman instrument was calibrated using the v1  
26 line of silicon at 520.7 cm<sup>-1</sup>.  
27  
28  
29  
30

31 Raman mapping was performed using a Jobin/Yvon LabRam 320 instrument  
32 equipped with an Olympus microscope (Horiba, Japan) by means of Ar<sup>+</sup> ion laser ( $\lambda = 532.8$   
33 nm) and 1800 l/nm grating on 3 different particles for each formulation. The experimental  
34 conditions were: 100 nm slit width, a 50× Microsoft objective and 0.4 s acquisition time.  
35 Each spectrum was the mean of the two. The sample profiling was performed at step  
36 increments of 3  $\mu$ m in the X–Y direction covering the biggest possible surface of the part.  
37 Principal component analysis (PCA) was applied to identify the number of components and  
38 plot the chemical maps. Prior to analysis, the spectra baseline was checked by using the  
39 automatic weighted least square and normalised to the unit area to avoid deviation among the  
40 Raman spectra.  
41  
42  
43  
44  
45  
46

### 47 **Taste masking of 3D designs**

48 In vivo taste masking evaluation was performed on 10 healthy human volunteers from  
49 whom informed consent was first obtained (approved by the Ethics Committee of the  
50 University of Greenwich). The study is also in accordance to the Code of Ethics of the World  
51 Medical Association (Declaration of Helsinki). The healthy volunteers of either sex (age 18–  
52 25) were selected, trained and the one Stramix design was held in the mouth for another 120  
53 s, and then spat out. The mouth was rinsed with water without swallowing the tablet. The  
54 equivalent of 50mg of bulk IND was held in the mouth for 30 s and then spat out. Bitterness  
55 was recorded immediately to the bitterness intensity scale from 1 to 5 where 1, 2, 3, 4, and 5  
56 indicate no, threshold, slight, moderate, and strong bitterness.  
57  
58  
59  
60  
61  
62  
63  
64  
65

## **In vitro dissolution studies**

Dissolution studies were conducted by using a USP II paddle apparatus (Varian 705, US). The amount of extruded powders was equivalent to 25 mg of IND, placed into 900 mL of phosphate buffer solution (pH 6.8), in each dissolution vessel (n = 3). The temperature of the dissolution media was maintained at 37 °C with a paddle rotation of 100 rpm. Samples, about 2–3 mL, were withdrawn at 10, 20, 30, 60, 90 and 120 min intervals and filtered with a 200 µm filter prior to HPLC analysis.

## **HPLC analysis**

The content of IND in dissolution samples was determined by HPLC. The samples were analysed on an HPLC system (Agilent Technologies, 1200 series) equipped with a quaternary pump using a Hichrom S50DS2-4889 (5 µm × 150 mm × 4 mm) column. The column temperature time was set at 25 °C while the retention time was 4 min. The mobile phase consisted of 70:30:0.2 (v/v/v) methanol/water/acetic acid and the injected sample volumes were 20 µL, the flow rate was 1.5 mL/min, and the detector was set at a wavelength of 260 nm. The calibration curve for IND was plotted over a concentration range of 10–50 µg/mL.

## **RESULTS AND DISCUSSION**

### **Hot melt extrusion (HME) and 3D printing coupling**

HME is a well-known processing pharmaceutical technology that has been successfully used over the past twenty years to increase the solubility of water insoluble drugs and mask the taste of bitter APIs for paediatric applications by producing solid dispersions [23]. In this study, HME was employed as the core technique to produce printing filaments and subsequently coupled with a 3D printer. HME nowadays is the predominant technique to create filaments of pharmaceutical compounds which can be subsequently inserted into the 3D printer. The active pharmaceutical ingredient (API) is introduced either by soaking [24] or by extrusion [25-27]. IND was selected as a model API as it has been previously reported to produce extruded solid dispersions with increased solubility while HPMCAS is a suitable thermoplastic carrier for manufacturing of drug loaded strands. The main aim of the study was to manufacture taste masked IND/HPMCAS solid dispersions with increase drug solubility in the form of strands/filaments that could be fed to the 3D printer and produce paediatric chewable tablets. According to Lopez et al., the capability of children to swallow solid dosage forms is a major issue and thus chewable tablets are an excellent paediatric dosage form [3]. They can be administered to children of 2 years old and older where swallowing or disintegration is assisted by the patient.

The design of the chewable tablets was inspired by the Starmix flavour gummy sweets (HARIBO plc.) to appear as “candy – like” formulations. By imitating these popular confectionaries the 3D printed chewable tablets aim to improve patient compliance and palatability.

## Process optimisation

Premixed drug, polymer and plasticiser blends were fed into the extruder in order to produce drug-loaded filaments suitable for 3D printing. One of the most critical features is the filament quality, which should be flexible enough to prevent any breakage printing. For that purpose, PEG was added as a plasticiser to facilitate better extrusion processing and enhance the strand flexibility. Various polymer/plasticiser ratios were tested (data not shown) to concluded that 20% PEG was giving the best filament quality. The diameter of the filament was adjusted between 2.7 and 2.9mm, to meet the 3D printer specifications. Due to the HPMCAS/PEG swelling at the end of the extrusion process a die of 1mm was selected to process the formulations.



*Fig. 1: Photographic image of the 3D printed medicines loaded with IND as model substance*

As shown in Fig. 1 various Starmix® IND loaded structures were printed at a wide range of designs. By using SolidWorks the process was programmed with 5% infill ratio  $25\text{mm s}^{-1}$  printing speed and  $160\mu\text{m}$  layer thickness in order to print doses of 25mg IND per structure. **The printing time for each Starmix® tablet was 5min.**

The 3D printing optimisation process was a prerequisite to achieving excellent bonding between the layers and thus fine 3D printed structures. All Starmix® structures were printed at temperatures of  $165^\circ\text{C}$  much higher than those used to extrude the exact same formulations. This can be explained by the effect of the extrusion process (e.g. screw configuration, temperature profile), which results in higher torque and consequently reduces significantly the melt viscosity of the extruded formulations. In addition, due to the small size of the 3D printing nozzle further temperature increase is required to reduce the melt viscosity of the filament and achieve the optimum printing conditions. Due to the complexity of the designs the weight of the individual printed forms was adjusted to deliver 50mg of IND according to the initial drug/polymer ratio. The 3D printing of Starmix® designs was

highly accurate, reproducible and produced smooth structures without any defects. Nevertheless, a weight and content uniformity variation of 5-10% was observed due the some inconsistencies of the filament thickness. The variations observed on tablet size were negligible.

### Scanning Electron Microscopy

The topography of the filament and the 3D printed structure was investigated by means of SEM. As illustrated in Fig 2a, the hot melt extruded filament presented a homogeneous and very smooth surface without any defects suggesting a perfect extrusion processing. No drug particles could be observed on the filament surface indicating very good IND blending and content uniformity (see further analysis). The manufacturing of high quality filaments is a prerequisite in order to facilitate robust 3D printing process with the required resolution of the printed designs. Fig. 2c shows the layer by layer deposition of the printed layers which appear to be uniform with close packing. The thickness of the layers were estimated at 150 - 180  $\mu\text{m}$ .

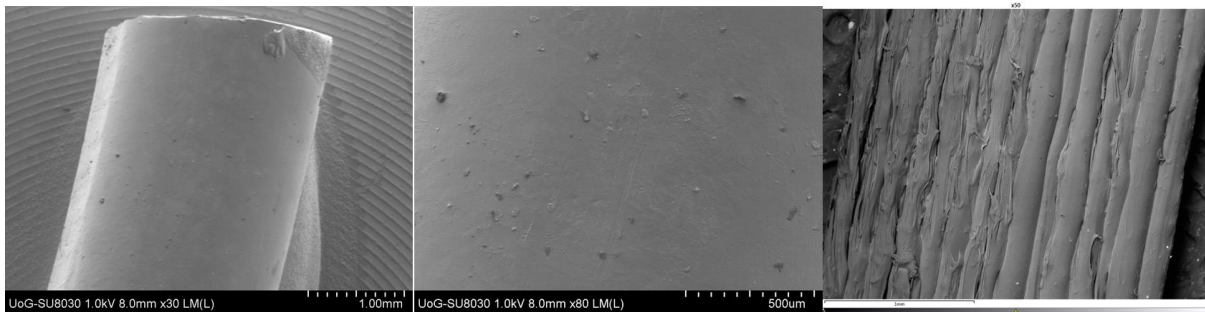


*Fig. 2: SEM images of a) extruded filament, b) surface of the extruded filament and c) surface of 3D structure*

### Thermal Analysis

Thermogravimetric analysis (TGA) was used to examine the thermal stability of pharmaceutical ingredients under the hot melt extrusion and 3D printing processing temperatures. In Fig. 3, IND showed that a negligible mass loss (0.5%) up to 170°C followed by a fast mass loss at around 220°C due to its degradation. AQOAT exhibited a small mass loss (2.7%) from 30 - 170°C and a second at 250°C which corresponds to its degradation. PEG was extremely stable at high temperatures without any losses and only presented a fast mass loss at 320°C due to its degradation. Both filament and the 3D printed Starmix structures demonstrates identical mass loss pathways showing that all mixtures remain stable up to 250°C with 2.8% mass loss, which is higher than the degradation temperature of IND indicating interactions among the polymers and the drug substance. Above this temperature, both samples exhibited a fast mass loss due to degradation. Overall, the TGA profiles demonstrate that the HME filament is suitable for 3D printing temperature at 165°C.

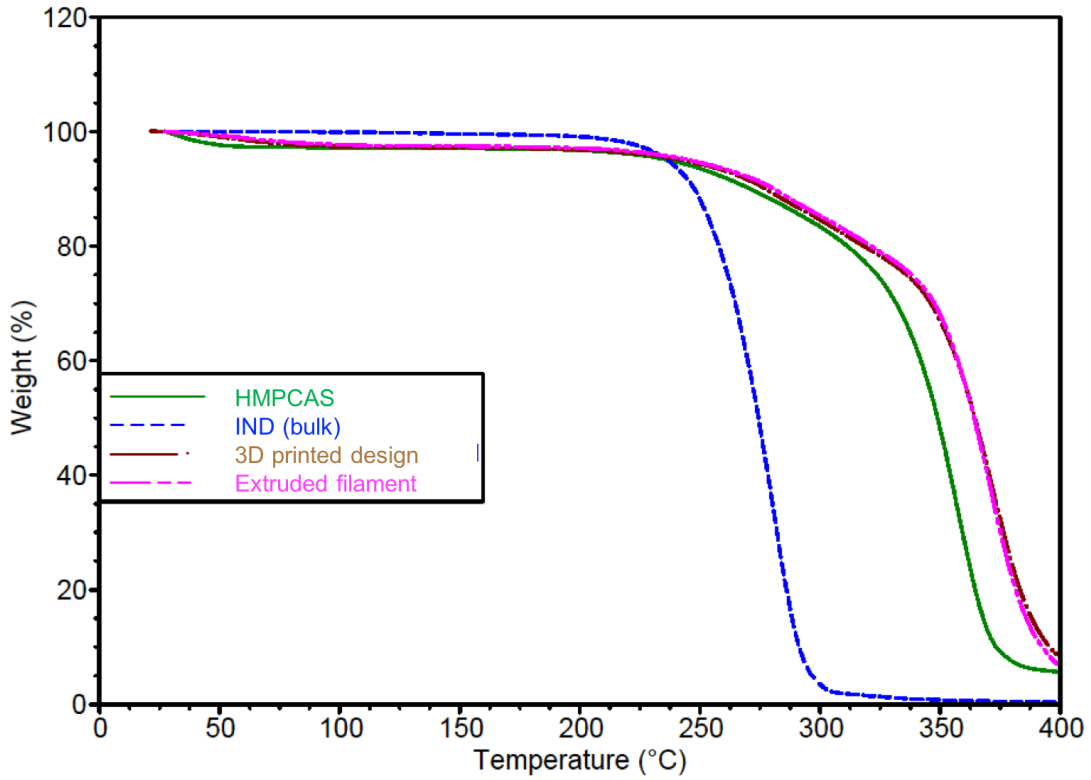


Fig. 3: TGA graph of the bulk IND, HPMCAS, PEG, extruded filament and 3D printed structure

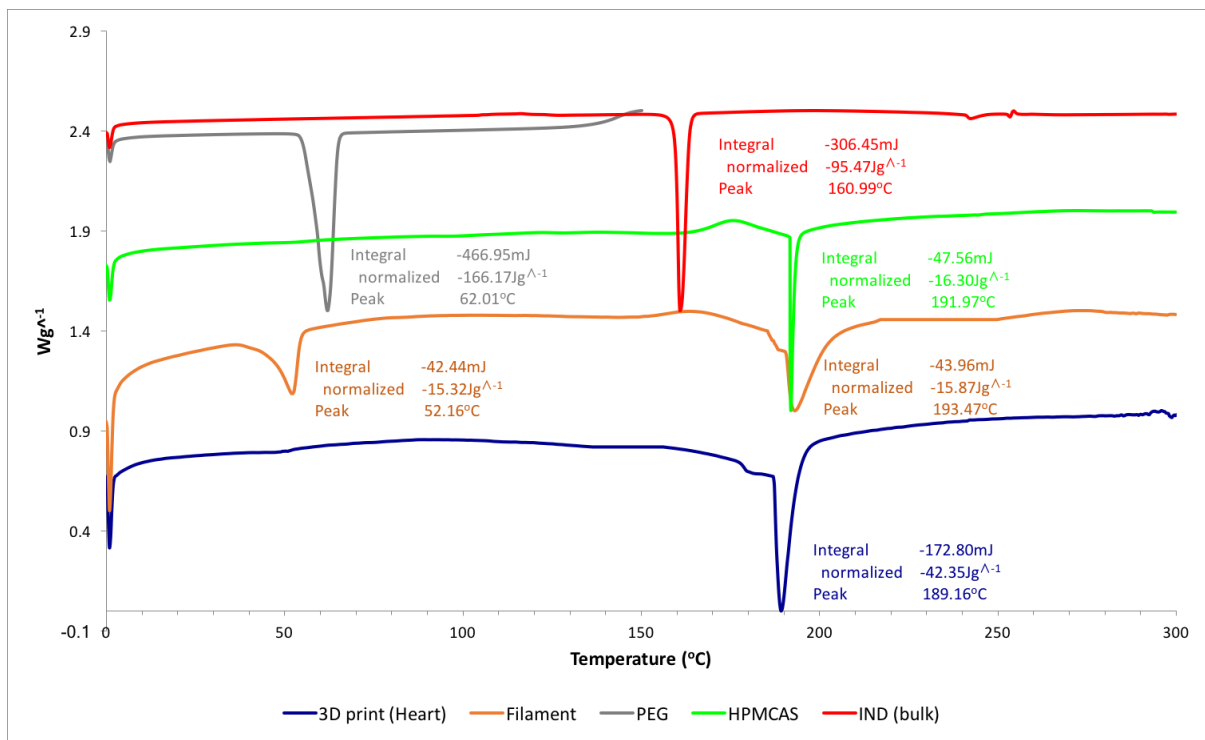


Fig. 4: DSC thermograph of pure IND, PEG, HPMCAS, extruded filament and 3D printed structure

DSC was conducted to investigate the physicochemical properties of the bulk materials the extruded filament and the 3D structures. As shown in Fig 4, IND exhibits a strong endothermic peak at 160.99°C which is typical for the crystalline  $\gamma$ -form while PEG 6000 exhibits a melting endotherm at 62°C. HPMCAS is an amorphous polymer with a glass transition at 131°C while it presents an exothermic peak at 175°C indicating crystallisation followed by a degradation endothermic peak at 191.8°C. The extruded filament shows a melting endotherm at 52.16° corresponding to PEG 6000 melting point suppression while no IND melting endotherm can be observed suggesting that the drug is in amorphous or molecularly dispersed form. A thermal endotherm appears at 223.5°C which is probably related to the HPMCAS degradation. Interestingly, in the thermogram of the 3D printed structures the PEG 6000 melting endotherm has disappeared suggesting that the polymer has turned to its amorphous state due to the second thermal processing (3D extrusion).

### X-Ray Diffraction analysis

X-ray analysis was performed in order to verify the physical state of IND in the 3D printed designs. The XRD diffractogram of bulk IND, HPMCAS, filament and 3D printed are illustrated in Fig. 5. The XRD of bulk IND presents strong intensity peaks at 11.6°, 16.4°, 19.6°, 26.89°, and 29.3° 2 $\theta$  values which correspond to  $\gamma$ -IND [28]. The HPMCAS diffractogram does not depict any intensity peaks due to the amorphous nature of the polymer, while PEG showed strong intensity peaks at 15° and 24°. The XRD of the extruded filament revealed two small peaks at 15° and at 24° 2 $\theta$  values, which are indicative of PEG suggesting that a part of the plasticiser is still in the crystalline state. This observation is also in good agreement with the DSC analysis where the PEG melting endotherm was identified. In contrast, the diffractograms of the 3D printed structure did not reveal any intensity peaks and the two PEG peaks have disappeared indicating that PEG has turned to completely amorphous state. This was attributed to the effect of the filament re-heating during the printing process, which occurs at higher temperature compared to the HME process.

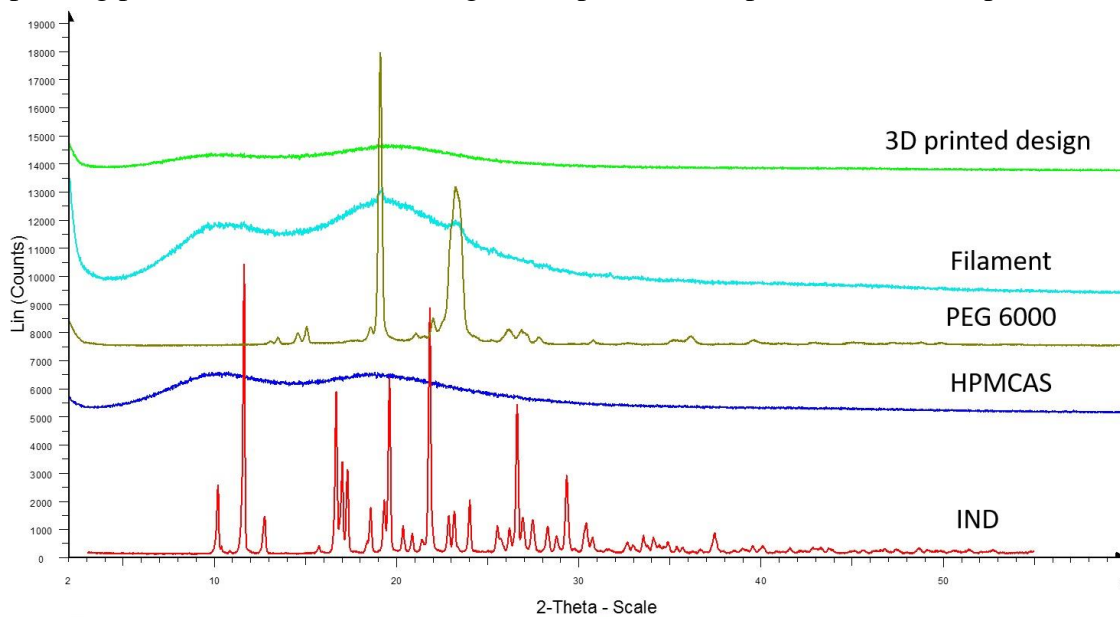
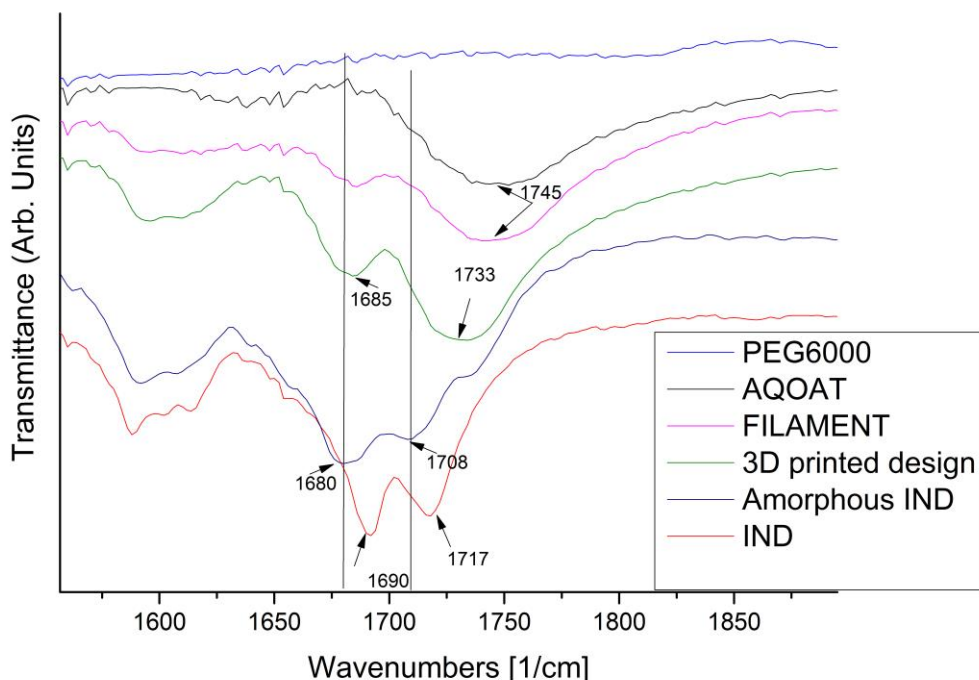


Fig. 5: XRD graphs of IND, HPMCAS, PEG, extruded filament and 3D printed structure

## FT-IR Spectroscopy

FT-IR analysis of the extruded formulations and the 3D printed structures was used to examine possible interactions among the compounds. Specifically, the carbonyl groups (-CO) and hydroxyl group (-OH) of IND can form hydrogen bonds with the -OH and COOH groups of AQOAT respectively. Such interactions of IND have previously reported with saccharin [29], polyvinyl pyrrolidone [30] and hydroxypropyl- $\beta$ -cyclodextrin [31]. The DSC and XRD analysis showed the presence of IND in amorphous form within the extruded filaments and printed structured. Therefore, amorphous IND was prepared in order to identify the related peak shifting compared to the crystalline form. Fig. 6 demonstrates that crystalline of  $\gamma$ -form indomethacin contains benzoyl and acid carbonyl groups corresponding at  $1717\text{cm}^{-1}$  and  $1690\text{cm}^{-1}$  respectively, whereas in amorphous form these peaks have moved towards lower wavenumbers at  $1708\text{cm}^{-1}$  (presence cyclic dimers) and  $1680\text{cm}^{-1}$  respectively. This observation is in good agreement with the published work by Taylor and Zografis [32]. In the 3D printed structure and filament the acid carbonyl group has moved to  $1685\text{cm}^{-1}$  whereas the benzoyl peak overlapped by the strong carbonyl peak of HPMCAS indicating H-bonding interactions. The amorphous state of IND in HPMC solid dispersions has also confirmed by other groups [33, 34], and it is attributed to the molecular mobility of IND within the polymer matrix. Another interesting observation is that the carbonyl peak of HPMCAS has shifted towards lower wavenumbers from  $1745\text{cm}^{-1}$  to  $1733\text{cm}^{-1}$  only for the 3D printed structure. This is due to the additional heat processing of the filament, suggesting stronger H-bonding interactions of the IND/HPMCAS blend.



**Fig. 6:** FT-IR graphs of PEG, HPMCAS, Filament, 3D printed mixture Amorphous IND and powder IND in the region of  $1550 - 1900\text{cm}^{-1}$

## Raman Mapping

Fig. 7 shows the Raman spectra of the bulk compounds, extruded filament and 3D printed structures in the range of  $1580\text{ cm}^{-1}$  –  $1700\text{ cm}^{-1}$  wavenumbers. Characteristic peaks of IND appear in the  $1580$  –  $1625\text{ cm}^{-1}$  region, HPMCAS at  $1740\text{ cm}^{-1}$  and PEG at  $1200$  –  $1300\text{ cm}^{-1}$ . Previous studies showed that the peak at  $1702\text{ cm}^{-1}$  corresponds to benzoyl carbonyl vibration while the peaks associated with the symmetrical stretching vibrations of the cyclic dimer formed by the carboxyl groups are not active in the Raman spectra [32]. In amorphous IND the peak is shifted towards lower wavenumbers at  $1684\text{ cm}^{-1}$ .

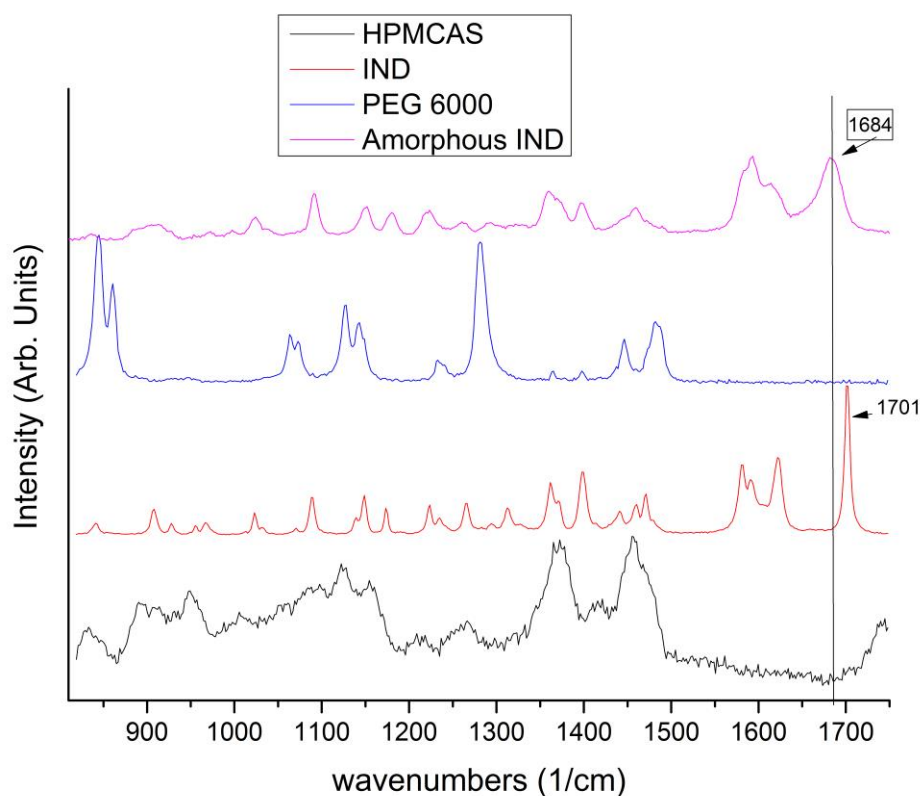


*Fig. 7: Raman Spectra of bulk HPMCAS, PEG 6000, crystalline and amorphous IND*

In order to investigate the IND homogeneity within the printed structures, multivariate data analysis PCA was applied to reduce the number of variables and identify the number of loadings, which consist the hyperspectral Raman data. Based on the eigenvalues, the hyperspectral data can be described by two principal components (PCs). This is a typical observation in multivariate data analysis of Raman spectra, which leads arbitrarily to the assumption that there are only two components in the system, as the first PC corresponds to the features of the strongest spectral contributors. It can be clearly observed from Fig. 8b that the peaks of the first PC correspond to characteristic of amorphous IND and HPMCAS in the formulation, which overwhelms the PEG's peaks. For instance, the characteristic pattern of IND peaks appears in the  $1550\text{ cm}^{-1}$  -  $1650\text{ cm}^{-1}$  region whereas several characteristic peaks of HPMCAS appear at  $1366\text{ cm}^{-1}$ ,  $1456\text{ cm}^{-1}$ , and  $1739\text{ cm}^{-1}$  wavenumber. The characteristic peaks of PEG appear in the 4<sup>th</sup> PC at  $840\text{ cm}^{-1}$  –  $885\text{ cm}^{-1}$  region and further at  $1236\text{ cm}^{-1}$ ,  $1282\text{ cm}^{-1}$  and at  $1486\text{ cm}^{-1}$  wavenumbers, whereas the intermediate PCs are attributed to the noise and are not represented. Furthermore, the peaks, of PC4 assigned to IND and HPMCAS

1  
2  
3  
4  
5  
6  
7  
8  
9  
10  
11  
12  
13  
14  
15  
16  
17  
18  
19  
20  
21  
22  
23  
24  
25  
26  
27  
28  
29  
30  
31  
32  
33  
34  
35  
36  
37  
38  
39  
40  
41  
42  
43  
44  
45  
46  
47  
48  
49  
50  
51  
52  
53  
54  
55  
56  
57  
58  
59  
60  
61  
62  
63  
64  
65

(Fig. 8b) at 1685  $\text{cm}^{-1}$  and 1739  $\text{cm}^{-1}$  respectively, confirm the homogeneity of the analysed samples. The Raman mapping analysis in Fig 2b showed that in the concentration maps (200  $\times$  200  $\mu\text{m}$ ) correspond to PC1 and PC4, IND is uniformly distributed in the bulk across the scanned areas while the coloured areas overlap indicating the existence of a molecular dispersion.

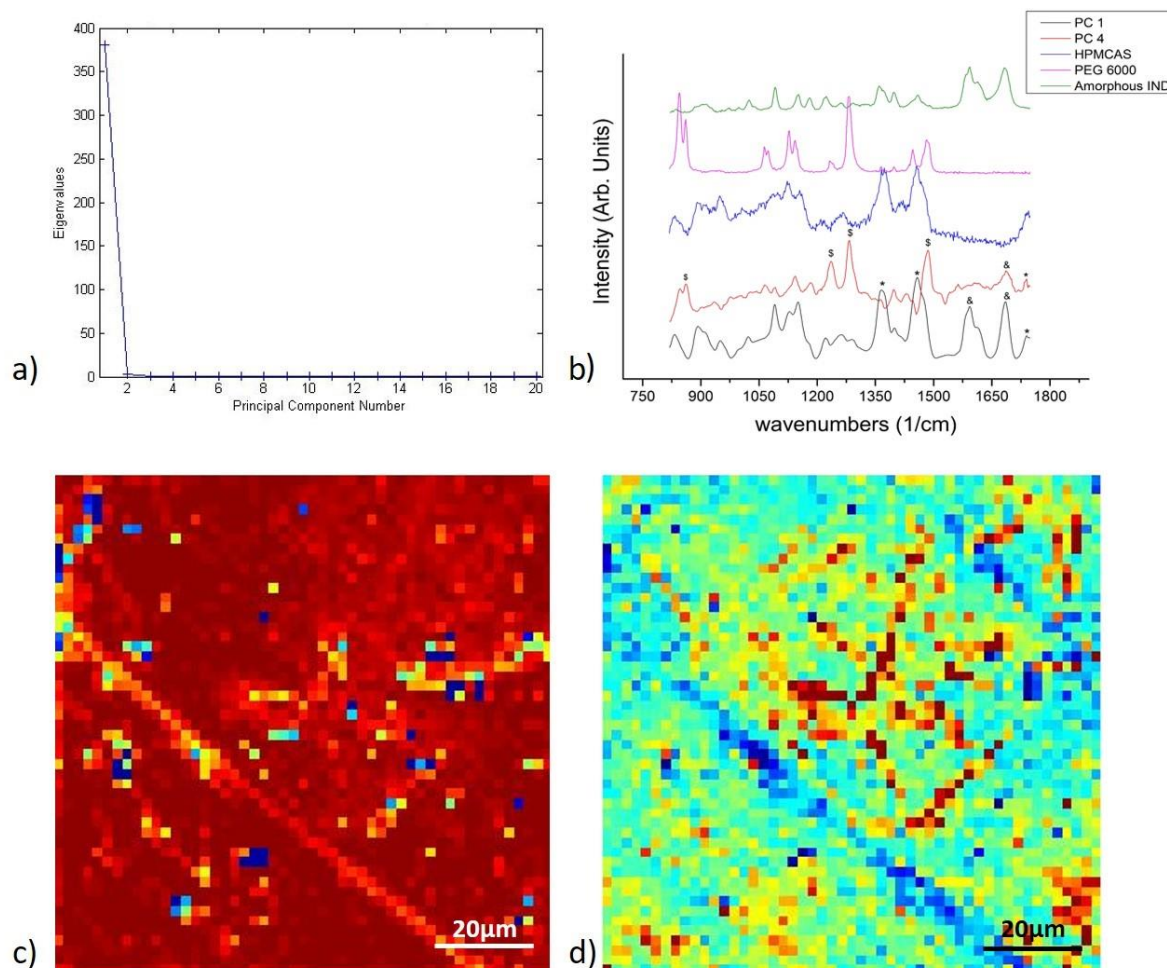


Fig. 8: a) Variation of Eigenvalues with the principal components, b) Comparison of HPMCAS and amorphous IND with the PC1 and PC4 where \$ correspond to PEG 6000, \* to HPMCAS and & to IND, c) Concentration map of PC1, d) Concentration map of PC4

### Taste masking evaluation

Taste masking efficiency of the 3D Starmix® designs was of the utmost importance for the purpose of paediatric applications [35, 36]. We anticipated that the selection of the excipients and the HME processing will result in efficient masking of IND bitterness and increase the palatability of the printed designs. As shown in Fig. 9 the panellist evaluation revealed moderate bitterness for IND while slight and threshold for PEG and HPMCAS respectively. All 3D printed designs showed excellent taste masking with no bitterness at all and no aftertaste was reported. The masking effect is attributed to the drug – polymer interactions through H- bonding facilitated by HME processing [37]. The effective taste

masking of the Starmix® designs suggests that 3D printed dosage forms can be successfully used in paediatric applications providing enhanced palatability.

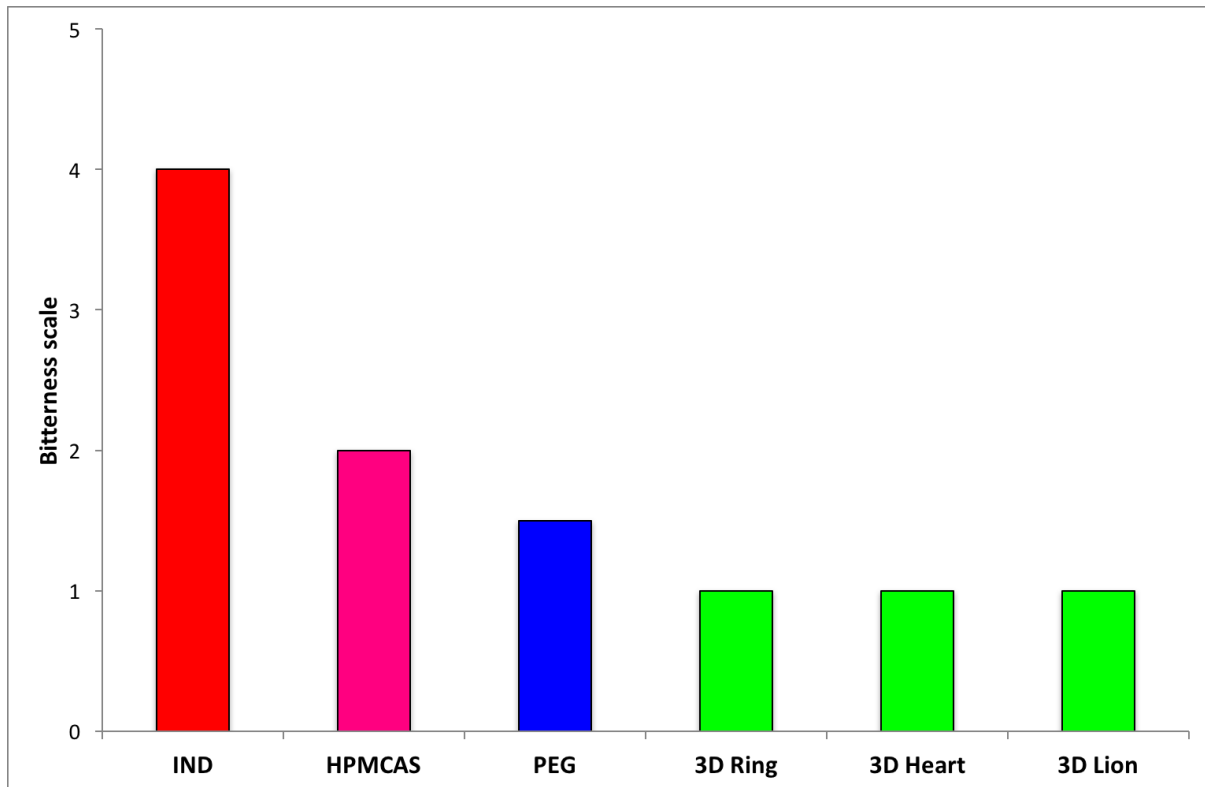


Fig. 9: Taste masking evaluation graph of bulk IND, HPMCAS, PEG and Starmix® designs

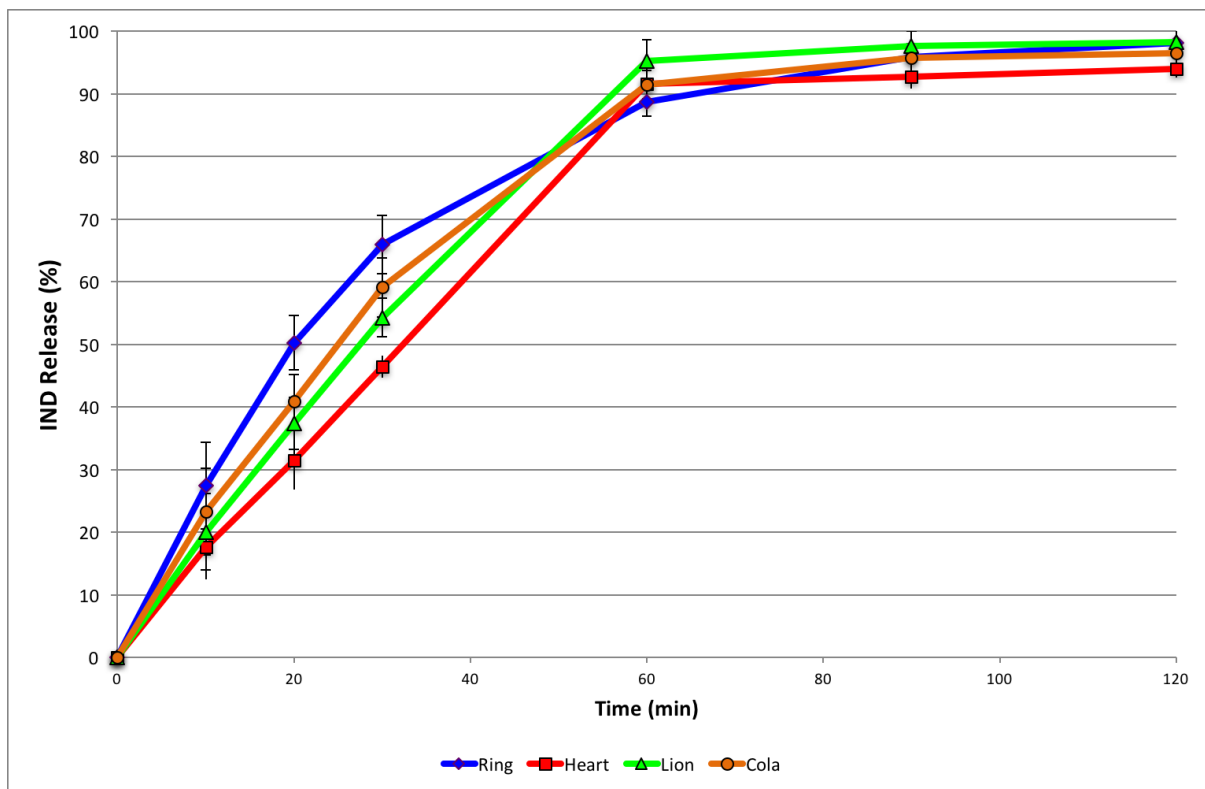


Figure 10: Dissolution rate of IND in three different 3D printed structure

## Dissolution studies

As HPMCAS dissolves at pH>6 we anticipated IND release in the mouth. However, children are expected to chew the tablets for a few minutes (up to 2min) and subsequently swallow them. For this reason, IND release was initially investigated similarly to Rachid et al by using small volumes (2ml) of simulated saliva (data not shown) [38]. The release of IND was found to vary from 8.0 – 12x10<sup>-3</sup>% which is negligible to cause any bitterness. These findings support the taste evaluation where the 3D printed tablets were found to mask IND bitterness.

In addition, the IND release profiles of four printed Starmix® designs were conducted in phosphate buffer (pH 7.4). The release profiles are illustrated in Fig 10 where it can be observed that for each printed form more than 80% of the drug was released within the first 60 min while the Starmix® designs were completely dissolved.

The rapid IND release was facilitated by the fact that HPMCAS is highly soluble in pH> 6.0 and IND is molecularly dispersed within the printed forms. Interestingly, the release profiles of all Stramix® designs are very similar and no significant difference was observed (p<0.05). It is also important to mention that the optimized printing process achieved release patterns independent of the printed designs. This is a crucial feature for the development of oral dosage forms with multiple designs or patterns. However, the alignment of drug release from 3D printed dosage forms was also observed by Goyanes *et al.* where tablets of different shapes and similar weights provided similar drug release profiles [20].

## CONCLUSION

Starmix® designs were manufactured by using FDM 3D printing coupled with HME processing for the development of palatable paediatric dosage forms. FDM process was proved efficient in printing detailed Starmix® designs with high reproducibility, accuracy and content uniformity. Physicochemical characterisation studies showed that IND was molecularly dispersed in the HPMCAS matrix. The panellist taste evaluation showed excellent taste masking efficiency and hence enhanced palatability. The drug release profiles showed rapid IND release independent of the shape of printed design. Overall, we demonstrated that 3D printing can be used as an alternative manufacturing route for paediatric medicines.

## REFERECNES

1. Strickley RG, Iwata Q, Wu S, Dahl TC. Pediatric drugs—a review of commercially available oral formulations, *Journal of pharmaceutical sciences*, 2008, 97:1731-1774.
2. Formulations of choice for the paediatric population. European Medicines Agency, (2006)
3. Lopez FL, Ernest TB, Tuleu C, Gul MO. Formulation approaches to pediatric oral drug delivery: benefits and limitations of current platforms, *Expert opinion on drug delivery*, 2015, 12:1727-1740.
4. Benavides S, Huynh D, Morgan J, Briars L. Approach to the pediatric prescription in a community pharmacy *J Pediatr Pharmacol Ther.* 2011, 16 (4):298-307.
5. Yin HS, Mendelsohn AL, Wolf MS, Parker RM, Fierman A, van Schaick L, Bazan IS, Kline MD, Dreyer BP. Parents' medication administration errors: role of dosing

instruments and health literacy, Archives of pediatrics & adolescent medicine, 2010, 164:181-186.

6. Mennella JA, Roberts KM, Mathew PS, Reed DR. Children's perceptions about medicines: individual differences and taste, BMC Pediatrics, 2015, 15:130.
7. Turner MA, Catapano M, Hirschfeld S, Giaquinto C Paediatric drug development: The impact of evolving regulations, Adv. Drug Deliv. Rev. 2014, 73:2-13.
8. Alhnan MA, Okwuosa TC, Sadia M, Wan KW, Ahmed W, Arafat B. Emergence of 3D Printed Dosage Forms: Opportunities and Challenges. Pharm Res. 2016 33(8):1817-32
9. Norman J, Madurawe RD, Moore CM, Khan MA, Khairuzzaman A. A new chapter in pharmaceutical manufacturing: 3D-printed drug products. Adv Drug Deliv Rev. 2017, 108:39-50
10. Sandler N, Preis M. Printed Drug-Delivery Systems for Improved Patient Treatment. Trends Pharmacol Sci. 2016, 37(12):1070-1080
11. Preis M, Öblom H. 3D-Printed Drugs for Children-Are We Ready Yet? AAPS PharmSciTech. 2017, 18(2):303-308
12. Sachs E, Cima M, Cornie J. Three-dimensional printing: rapid tooling and prototypes directly from a CAD model, CIRP Ann Manuf, Techn. 1990, 39: 201-204.
13. Khaled SA, Burley JC, Alexander MR, Roberts CR. Desktop 3D printing of controlled release pharmaceutical bilayer tablets, Int. J. Pharm. 2014,461:105-111.
14. Goyanes A, Chang H, Sedough D, Hatton GB, Wang J, Buanz A, Gaisford S, Basit AW. Fabrication of controlled-release budesonide tablets via desktop (FDM) 3D printing, Int. J. Pharm. 2015, 496:414-420.
15. Water JJ, Bohr A, Boetker J, Aho J, Sandler N, Nielsen HM, Rantanen J. Three-Dimensional Printing of Drug-Eluting Implants: Preparation of an Antimicrobial Polylactide Feedstock Material. J. Pharm. Sci. 2015, 104:1099-1107.
16. Khaled SA, Burley JC, Alexander MR, Yang J, Roberts CJ. 3D printing of five-in-one dose combination polypill with defined immediate and sustained release profiles. J. Control. Rel. 2015, 217:308-314.
17. Goyanes A, Det-Amornrat U, Wang J, Basit AW, Gaisford S. 3D scanning and 3D printing as innovative technologies for fabricating personalized topical drug delivery systems. J. Control. Rel., 2016, 234:41-48.
18. Busch SF, Weidenbach M, Fey M, Schäfer F, Probst T, Koch M. Optical Properties of 3D Printable Plastics in the THz Regime and their Application for 3D Printed THz Optics. J Infrared Millim Terahertz Waves. 2014,35:993-997.
19. Goyanes A, Buanz A, Hatton GB, Gaisford S, Basit AW. 3D printing of modified-release aminosaliclylate (4-ASA and 5-ASA) tablets. Eur. J. Pharm. Biopharm. 2015, 89:157-162.
20. Goyanes A, Martinez PR, Buanz A, Basit AW, Gaisford S. Effect of geometry on drug release from 3D printed tablets. Int. J. Pharma. 2015, 494: 657-663.
21. Skowrya J, Pietrzak K, Alhnan MA Fabrication of extended-release patient-tailored prednisolone tablets via fused deposition modelling (FDM) 3D printing. Eur. J. Pharm. Sci. 2015, 68:11-17.
22. Okwuosa TC, Stefaniak, D Arafat B, Isreb A, Wan K-W, Alhnan MA. A Lower Temperature FDM 3D Printing for the Manufacture of Patient-Specific Immediate Release Tablets. Pharm Res. 2016, 33(11):2704-12
23. Maniruzzaman M, Boateng JB, Bonnefille M, Aranyos A, Mitchell JC, Douroumis D. Taste masking of paracetamol by hot-melt extrusion: An in vitro and in vivo evaluation. Eur. J. Pharm. Biopharm. 2012, 80: 433-442.

- 1 24. Goyanes A, Buanz AB, Basit AW, Gaisford S. Fused-filament 3D printing (3DP) for  
2 fabrication of tablets. *Int. J. Pharma.* 2014, 476: 88-92.
- 3 25. Genina N, Holländer J, Jukarainen H, Mäkilä E, Salonen J, Sandler N. Ethylene vinyl  
4 acetate (EVA) as a new drug carrier for 3D printed medical drug delivery devices.  
5 *Eur. J. Pharm. Sci.* 2015, 30(90):53-63
- 6 26. Melocchi A, Parietti F, Maroni A, Foppoli A, Gazzaniga A, Zema L. Hot-melt  
7 extruded filaments based on pharmaceutical grade polymers for 3D printing by fused  
8 deposition modelling. *Int. J. Pharm.* 2016, 509: 255-263.
- 9 27. Boetker J, Water JJ, Aho J, Arnfast L, Bohr A, Rantanen J. Modifying release  
10 characteristics from 3D printed drug-eluting products. *Eur. J. Pharm. Sci.* 2016, 90:  
11 47-52.
- 12 28. El-Badry M, Fetih G, Fathy M. Improvement of solubility and dissolution rate of  
13 indomethacin by solid dispersions in Gelucire 50/13 and PEG4000, *Saudi Pharm. J.*  
14 2009, 17: 217-225.
- 15 29. Zhang G-C, Lin H-L, Lin S-Y. Thermal analysis and FTIR spectral curve-fitting  
16 investigation of formation mechanism and stability of indomethacin-saccharin  
17 cocrystals via solid-state grinding process. *J. Pharm. Biomed. Anal.* 2012, 66:162-  
18 169.
- 19 30. Lim RTY, Ng WK, Tan RB. Dissolution enhancement of indomethacin via  
20 amorphization using co-milling and supercritical co-precipitation processing, *Powder*  
21 *Tech.* 2013, 240: 79-87.
- 22 31. Bandi N, Wei W, Roberts CB, Kotra LP, Kompella UB. Preparation of budesonide-  
23 and indomethacin-hydroxypropyl- $\beta$ -cyclodextrin (HPBCD) complexes using a  
24 single-step, organic-solvent-free supercritical fluid process. *Eur. J. Pharm. Sci.* 2004,  
25 23:159-168.
- 26 32. Taylor LS, Zografi G Spectroscopic Characterization of Interactions Between PVP  
27 and Indomethacin in Amorphous Molecular Dispersions. *Pharm. Res.* 1997, 14:1691-  
28 1698.
- 29 33. Ewing AV, Clarke GS, Kazarian SG. Stability of indomethacin with relevance to the  
30 release from amorphous solid dispersions studied with ATR-FTIR spectroscopic  
31 imaging. *Eur. J. Pharm. Sci.* 2014, 60: 64-71.
- 32 34. Chauhan H, Kuldipkumar A, Barder T, Medek A, Gu C-H, Atef E. Correlation of  
33 Inhibitory Effects of Polymers on Indomethacin Precipitation in Solution and  
34 Amorphous Solid Crystallization Based on Molecular Interaction. *Pharm. Res.* 2014,  
35 31:500-515.
- 36 35. Walsh J, Cram A, Woertz K, Breitzkreutz J, Winzenburg G, Turner R, Tuleu C, E.F.  
37 Initiative, Playing hide and seek with poorly tasting paediatric medicines: do not  
38 forget the excipients, *Adv. Drug Deliv. Rev.* 2014, 73:14-33.
- 39 36. Maniruzzaman M, Boateng JS, Chowdhry BZ, Snowden MJ, Douroumis D. A review  
40 on the taste masking of bitter APIs: hot-melt extrusion (HME) evaluation. *Drug Dev.*  
41 *Ind. Pharm.* 2014, 40:145-156.
- 42 37. Gryczke A, Schminke S, Maniruzzaman, Beck MJ, Douroumis D. Development and  
43 evaluation of orally disintegrating tablets (ODTs) containing Ibuprofen granules  
44 prepared by hot melt extrusion. *Colloids Surf. B: Biointerfaces.* 2011, 86: 275-284.
- 45 38. Rachid Q, Rawas-Qalaji M, Estelle F, Simons R, Simons KJ. Dissolution Testing of  
46 Sublingual Tablets: A Novel In Vitro Method. *AAPS PharmSciTech.* 2011, 12(2):  
47 544-552.
- 48
- 49
- 50
- 51
- 52
- 53
- 54
- 55
- 56
- 57
- 58
- 59
- 60
- 61
- 62
- 63
- 64
- 65